

An Advanced Loop Heat Pipe for Cryogenic Applications

Jentung Ku ¹

NASA Goddard Space Flight Center, Greenbelt, Maryland, 20771, USA

Triem Hoang ²

TTH Research, Inc., Clifton, Virginia 20124, USA

A loop heat pipe (LHP) is a very versatile heat transfer device that can transport a large heat load over a long distance with a small temperature difference. All LHPs currently servicing orbiting spacecraft are designed to operate in the room temperature range. Future space telescopes and space-based Earth resource imaging satellites require passive cryogenic heat transport devices that can thermally couple remote cryocoolers to sensor or instrument of interest while providing the capability of payload vibration/jitter isolation, implementation of redundant coolers, and coupling of multiple sensors to a common heat sink. All of these requirements can be satisfied by using a cryogenic LHP (CLHP). Although the development of CLHPs faces several technical challenges, NASA Goddard Space Flight Center has devoted extensive efforts in developing CLHP technology over the past decade and has made significant progress. In particular, the combination of innovative ideas of using a secondary capillary pump to manage the parasitic heat gain and using a hot reservoir to reduce the system pressure under the ambient condition has led to the successful development of the CLHP. Several CLHPs charged with nitrogen and hydrogen were built and tested in thermal vacuum chambers. These CLHPs demonstrated reliable start-up and robust operation during power cycle and sink temperature cycle tests.

Nomenclature

CC	= compensation chamber
CLHP	= cryogenic loop heat pipe
CTE	= coefficient of thermal expansion
GSFC	= Goddard Space Flight Center
LHP	= loop heat pipe
NASA	= National Aeronautics and Space Administration
SBIR	= Small Business Innovative Research
$C_{p,l}$	= specific heat of liquid [J/kg-K]
$G_{E,CC}$	= thermal conductance between primary evaporator and CC [W/K]
m_1	= mass flow rate in the primary loop [kg/s]
m_2	= mass flow rate in the secondary loop [kg/s]
Q_{CC}	= heat exchange between CC and environment [W]
Q_{COND}	= heat dissipation by condenser [W]
Q_E	= primary evaporator heat input used to vaporize liquid [W]
Q_{High}	= highest heat load for LHP to be controlled at a given temperature [W]
Q_{IN}	= external heat input to the primary evaporator [W]
Q_{Leak}	= heat leak from evaporator to CC [W]
Q_{Low}	= lowest heat load for LHP to be controlled at a given temperature [W]
q_{IN}	= external heat input to the secondary evaporator [W]
T_{CC}	= compensation chamber temperature [K]
T_E	= evaporator temperature [K]

¹ Lead Aerospace Engineer, Thermal Engineering Branch, Code 545, NASA/GSFC, Greenbelt, MD 20771

² President, TTH Research, Inc., 7830 My Way, Clifton, VA, 20124

T_{IN}	= temperature of returning liquid entering the reservoir [K]
$T_{IN,2}$	= temperature of returning liquid entering the secondary evaporator [K]
ΔT_{SUB}	= amount of liquid subcooling to the primary loop [K]
x_{OUT}	= quality of flow from CC to secondary evaporator
λ	= latent heat of vaporization [J/kg]

I. Introduction

A LOOP heat pipe (LHP) is a very versatile heat transfer device which can transport a large heat load over a long distance with a small temperature difference [1-3]. It utilizes boiling and condensation of the working fluid to transfer heat, and the surface tension forces of menisci formed at the liquid/vapor interfaces on the porous wick to sustain the pressure drop induced by the fluid flow. As shown in Figure 1, a typical LHP consists of an evaporator pump with an integral reservoir (also known as compensation chamber or CC), a condenser, a vapor line and a liquid line. The evaporator contains a primary porous wick which separates the vapor on the outer surface from the fluid in the evaporator inner core, and a secondary wick which connects the evaporator inner core to the reservoir. The rest of the loop is made of smooth tubes. The operating principles of an LHP can be found in the literature [1-3]. There are different terms used to describe the same item in the literature. In this paper, the terms reservoir and compensation chamber (CC) will be used interchangeably. Likewise, the terms evaporator and pump will be used interchangeably.

LHPs are being used on several commercial communications satellites and NASA's ICESat, Swift, Aura, GOES-N and GOES-R spacecraft [4-11]. These LHPs were designed to operate in the room temperature range. Future space telescopes and space-based Earth resource imaging satellites require passive cryogenic heat transport devices that can thermally couple remote cryocoolers to the sensor or instrument of interest while providing the capability of payload vibration/jitter isolation, implementation of redundant coolers, and coupling of multiple sensors to a common heat sink. All of these requirements can be satisfied by using a cryogenic LHP (CLHP).

As will be elaborated on later, the development of CLHPs faces several technical challenges, including: 1) start-up of the CLHP from a supercritical state; 2) parasitic heat gains along the liquid return line; 3) containment of the system pressure at the room temperature; and 4) a mismatch of coefficients of thermal expansion (CTE) between the wick and the evaporator shell. Over the past decade or so, NASA/GSFC has devoted extensive efforts to the development of CLHPs through the Small Business Innovative Research (SBIR) program. In particular, the advanced CLHP concept employing a secondary evaporator and a hot reservoir can overcome all of the above-mentioned CLHP technical challenges. Several advanced CLHPs have been built using different working fluids, and all of them demonstrated excellent performance.

The concept of the advanced CLHP will be presented first along with its operating principles and techniques used to overcome the CLHP technical challenges. This will be followed by a description of the design and testing of a hydrogen CLHP as an example.

II. Concept of Advanced CLHP and Its Operating Principles

2.1 Technical Challenges of the CLHP

The CLHP must start successfully before it can commence its service. The start-up and subsequent operation of the CLHP requires that both liquid and vapor of the working fluid be present in the evaporator and reservoir. The fluid in the entire CLHP is usually in a supercritical state prior to start-up. The condenser can be cooled relatively quickly due to its direct exposure to the cold sink such as the cold finger of a cryocooler. On the other hand, cooling of the evaporator and reservoir will be very slow because they are located remotely from the heat sink. Thus, liquid will form in the condenser first when the condenser temperature is colder than the

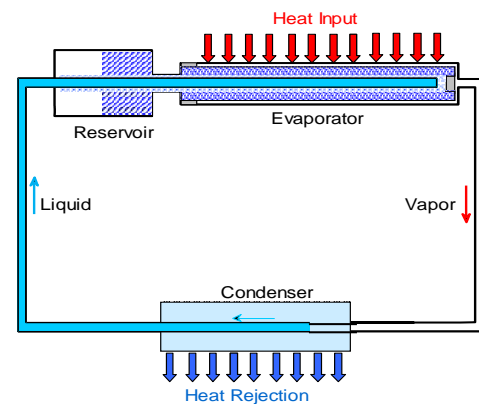


Figure 1. Schematic of a Typical LHP

critical temperature and the loop pressure is lower than the critical pressure of the working fluid. Once liquid is formed in the condenser, the evaporator and the reservoir can be cooled effectively from a superheated state to a saturation state by circulating the liquid around the loop. However, the circulation of fluid requires a driving force, and the usual driving force provided by the surface tension force in the evaporator wick is not yet available prior to the loop start-up.

The CLHP must be charged with a minimum amount of fluid in order to operate in the cryogenic temperature range. At the ambient temperature, the fluid will be at a supercritical state and its pressure can be as high as 15 to 22 MPa (~2000 to 3000 psi). Although the CLHP shell can be made very thick to contain the high pressure, most flight projects regard this as a safety risk during processing and handling of the CLHP. More importantly, unless the loop pressure can be lowered below the critical pressure, no liquid can be formed anywhere in the loop, not even in the condenser where the local temperature has been cooled below the critical temperature. Some measures are needed to lower the loop pressure below the critical pressure to ensure the liquid formation in the condenser prior to engaging the loop start-up process.

During the CLHP operation, there is an internal heat leak from the evaporator to the reservoir. In addition, the reservoir may have parasitic heat gains from its surroundings. The heat leak and parasitic heat gain are compensated by subcooling of the liquid returning from the condenser in traditional LHPs [12, 13]. For CLHPs, such liquid subcooling can rapidly diminish as the liquid flows along the liquid line which is exposed to surrounding at a much higher temperature. This is especially true at load heat loads where the mass flow rate is small and the fluid particles have a long resident time in the liquid line. How to overcome the heat leak from the evaporator and parasitic heat gains from the environment is a critical issue for the CLHP operation.

The primary wick inside the evaporator must be in close contact with the evaporator shell in order to maintain a low thermal resistance. A tight seal is also required in order to prevent the vapor at the outer surface of the primary wick from penetrating into the liquid core of the evaporator. A mismatch in the CTEs between the primary wick and the evaporator shell over the range from the ambient temperature to cryogenic temperature could affect the required tightness of the seal between the two components. The possible CTE mismatch is another issue that must be resolved in the design of the CLHP.

2.2 The Concept of Advanced CLHP

Figure 2 shows the flow schematic of an advanced CLHP [14-16] which can overcome the four technical challenges faced by the CLHP. The main feature of the advanced CLHP concept is the incorporation of a secondary evaporator and a hot reservoir into the traditional LHP. The secondary evaporator is located in a cold-biased environment to ensure that its wick is always primed. It connects to the regular reservoir via a secondary fluid line, and to the main vapor line via a secondary vapor line. The primary functions of the secondary evaporator are: 1) to maintain the reservoir saturation temperature by managing the heat leak from the evaporator and the parasitic heat gains from the environment as liquid flows along the liquid return line; and 2) to ensure a successful start-up of the loop. The fluid flow from the secondary evaporator through primary condenser, primary liquid line, reservoir, and secondary fluid line forms a secondary loop. When the secondary evaporator receives no net heat load and becomes inactive, the function of the advanced CLHP degenerates to that of the traditional LHP, which is termed the primary loop here. The hot reservoir is used to reduce the system pressure under ambient condition, and must be large enough to ensure that the system pressure is lower than the critical pressure of the working fluid prior to CLHP startup. The hot reservoir will be in thermal equilibrium with ambient, and there is no need to control its temperature. As the operating condition of the CLHP changes, there is mass exchange between the CLHP and the hot reservoir.

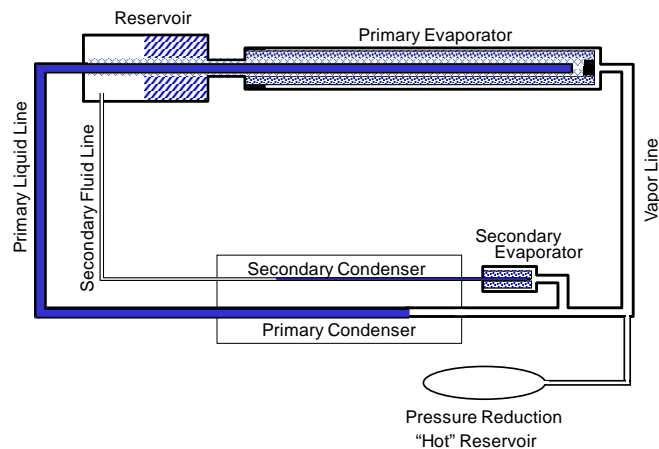


Figure 2. Flow Schematic of an Advanced CLHP

The operating temperature at which liquid vaporizes in the primary evaporator is governed by the saturation temperature of the working fluid in the reservoir. The reservoir saturation temperature is a result of energy balance between the subcooling of liquid returning from the condenser and heat gains including heat leak from the evaporator and parasitic heat. The liquid subcooling and heat leak are functions of the heat load to the evaporator, condenser heat sink temperature, and the ambient temperature along the liquid line [2, 12]. For a traditional LHP with a well-insulated reservoir and for a given condenser sink temperature that is lower than the ambient temperature, the reservoir saturation temperature as a function of the evaporator heat load yields a V-shape curve as shown in Figure 3. This is defined as the LHP natural operating temperature. The reservoir temperature can be controlled at a desired temperature by using a control heater for heat loads between Q_{low} and Q_{high} because the LHP natural operating temperature is lower than the desired set point temperature. This is the essence of cold-biasing in LHP operating temperature control. For heat loads below Q_{low} , the natural operating temperature is higher than the desired set point temperature and some active means of cooling the reservoir is required in order to maintain the desired reservoir set point temperature. For CLHP, the parasitic heat gained by the liquid along the liquid line can be so large that the liquid loses all subcooling and becomes two-phase fluid. The operating temperature of the CLHP may keep rising until it exceeds the critical temperature of the working fluid, and the CLHP will cease to function.

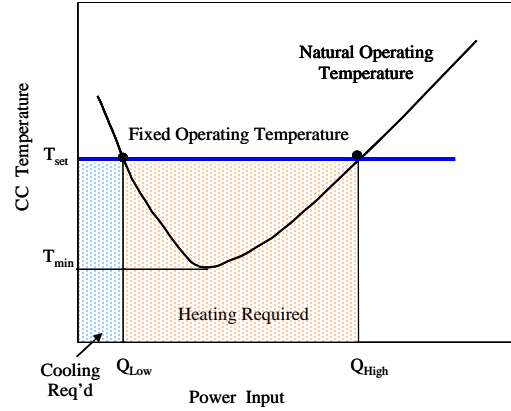


Figure 3. LHP Operating Temperature Control

When the secondary evaporator in the CLHP is operational, it takes heat out of the reservoir by removing two-phase fluid from the reservoir. Thus, the secondary evaporator works as an active cooling device for the reservoir. Figure 4 shows the operation of the advanced CLHP. The advantage offered by the CLHP in managing the parasitic heat gains is best illustrated by looking into the governing equations for heat transfer.

During the operation of a traditional LHP where the secondary evaporator and the hot reservoir are absent, the heat applied to the primary evaporator Q_{IN} is divided into two parts [17]: an amount of Q_E is used to vaporize the liquid to generate a mass flow rate of m_1 , and the remainder is transmitted through the primary wick to the reservoir as a heat leak, i.e.

$$Q_{IN} = Q_E + Q_{Leak} \quad (1)$$

$$Q_E = m_1 \lambda \quad (2)$$

$$Q_{Leak} = G_{E,CC} (T_E - T_{CC}) \quad (3)$$

The heat leak from the primary evaporator to the reservoir plus any heat gains by the reservoir must be balanced by the subcooling carried by the liquid returning to the reservoir:

$$Q_L + Q_{CC} = m_1 C_{p,l} \Delta T_{SUB} \quad (4)$$

$$\Delta T_{SUB} = T_{CC} - T_{IN} \quad (5)$$

When the traditional LHP is operating in the cryogenic temperature range, the parasitic heat gain by the returning liquid from its hot surrounding can result in liquid boiling in the liquid line, i.e. $\Delta T_{SUB} = 0$, and there is no subcooling liquid to compensate for the heat gains. The reservoir temperature can keep going up until it is higher than the critical temperature, rendering the LHP inoperable.

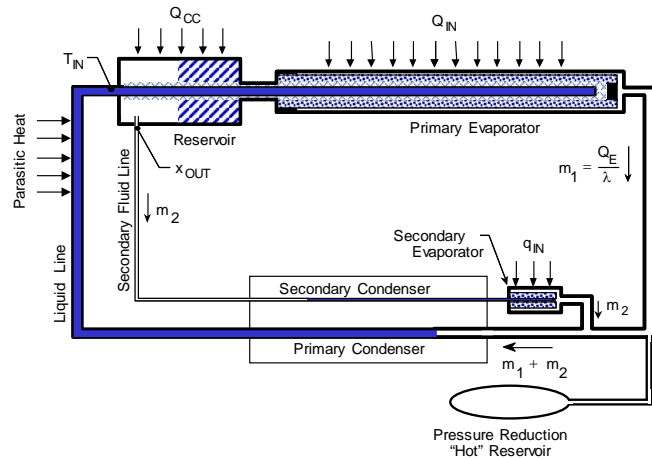


Figure 4. Management of CLHP Heat Gains

With an advanced CLHP, a heat load of q_E can be applied to the secondary evaporator to generate a mass flow rate of m_2 :

$$Q_{IN} = m_2[\lambda + C_{p,l}(T_{CC} - T_{IN,2})] \quad (6)$$

The energy balance for the reservoir can be re-written as:

$$Q_L + Q_{CC} = m_1 C_{p,l} \Delta T_{SUB} + m_2 C_{p,l} \Delta T_{SUB} + m_2 \lambda x_{OUT} \quad (7)$$

The effect of applying q_{IN} to the secondary evaporator is clearly seen in equation (7). The second term on the right side is the additional subcooling entering the reservoir, whereas the third term is the amount of heat removed from the reservoir. The heat removed from the reservoir is dissipated into the secondary condenser. Thus, the secondary evaporator serves as an active cooler to cool the reservoir.

In addition to managing parasitic heat gains, the ability of the secondary evaporator to remove heat from the reservoir proves particularly useful for the loop start-up. Initially, the entire CLHP is full of supercritical vapor. When the cryocooler is activated, the primary condenser, secondary condenser, and secondary evaporator all decrease in temperature until they reach the cryocooler set point temperature, which is lower than the critical temperature of the working fluid. When the loop pressure is also lower than the critical pressure of the working fluid, liquid will form in the condensers and secondary evaporator but nowhere else. The condition is depicted in Figure 5, where the hot reservoir is not shown. At this time, heaters attached to the secondary evaporator are turned on to initiate a fluid circulation in the secondary loop, i.e. vapor generated in the secondary evaporator flows to the primary condenser and condenses into liquid, and liquid moves from the primary condenser to the primary evaporator (via the bayonet tube) and reservoir, and is eventually drawn from the reservoir back to the secondary condenser and secondary evaporator. This is shown in Figure 6. When temperatures of the liquid line and primary evaporator become subcritical, liquid will be formed in those places. The CLHP is finally ready for start-up and power can be applied to the primary evaporator as shown in Figure 7.

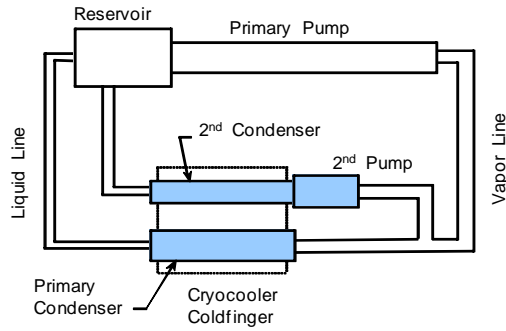


Figure 5. CLHP start-up: cryocooler cooldown and liquid formation

The problem of the CTE mismatch can be solved by using the same material for the primary evaporator and its wick. For example, stainless steel wick with pore size on the order of $1 \mu\text{m}$ has been developed, and the stainless steel evaporator shell has an adequate thermal conductivity for heat transfer between the heat source and the CLHP.

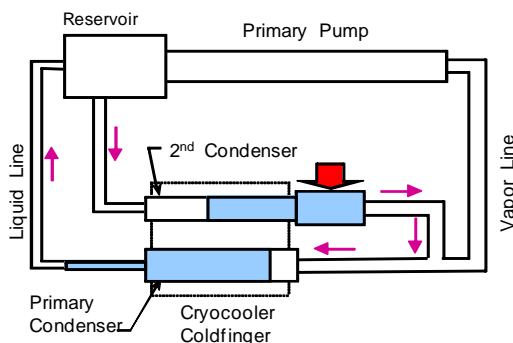


Figure 6. CLHP start-up: cooling and priming the primary evaporator

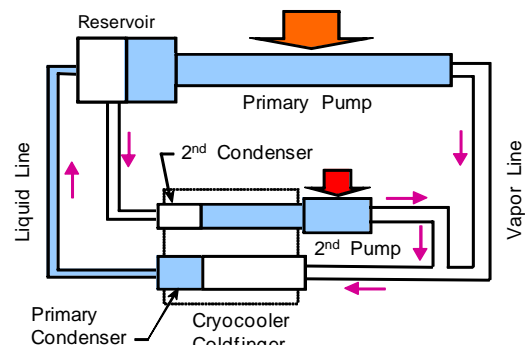


Figure 7. CLHP start-up: applying power to the primary evaporator

Several CLHPs have been built and filled with nitrogen and hydrogen, and have been successfully tested in thermal vacuum chambers to demonstrate the operation for temperature around 80K and 22K, respectively. The following section describes the design and testing of a hydrogen CLHP.

III. Testing of a Hydrogen CLHP

Under the NASA SBIR program, TTH Research, Inc. has built and tested a proof-of-concept advanced CLHPs using hydrogen as the working fluid to demonstrate the feasibility of such as design [14, 15, 18]. Figures 8 and 9 show the component layout and picture of the hardware of a hydrogen advanced CLHP, respectively. Major design parameters are shown in Table 1. All LHP components are made of stainless steel.

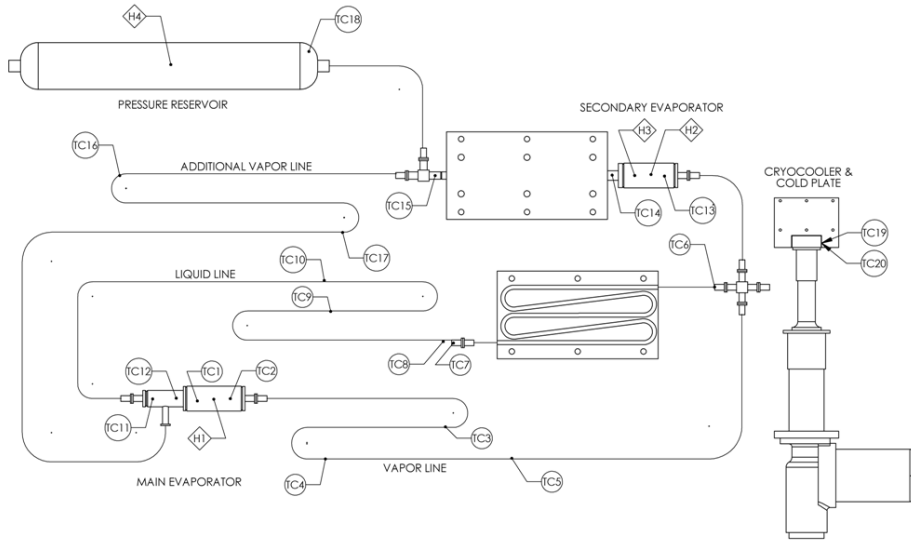


Figure 8. Component Layout of Hydrogen CLHP

Table 1. Design Parameters of Proof-of-Concept Hydrogen CLHP

Component	Dimensions
Primary Evaporator	19mm OD x 25.4mm L
Primary Wick	3 micron pore radius, 45% porosity, $0.5 \times 10^{-13} \text{ m}^2$ permeability
Reservoir	19 mm OD x 25.4mm L
Secondary Evaporator	19 mm OD x 25.4mm L
Wick in Secondary Evaporator	3 micron pore radius, 45% porosity, $0.5 \times 10^{-13} \text{ m}^2$ permeability
Vapor Line	3.2mm OD x 2.4mm ID x 2500mm L
Liquid Line	2mm OD x 1.6mm ID x 2500mm L
Additional Vapor Line	2mm OD x 1.6mm ID x 2500 L
Serpentine Condenser Length	3.2mm OD x 1.6mm ID x 813mm L
Length through 2 nd Condenser	6.4mm OD x 4.9mm ID x 6152mm L
Pressure Reduction Reservoir	101.6mm OD x 91mm ID x 678mm L

The hydrogen advanced LHP was mounted in a stainless steel frame. The test article was placed inside a 752 mm (30 inches) diameter x 3.05 m (10-foot) length thermal vacuum chamber for performance tests. A Kapton-backed foil heater was bonded to the primary evaporator to simulate the heat load. The evaporators were insulated with MLI blankets. The main condenser was a copper plate with an area of 76mm x 139.7 mm with a serpentine line brazed to it. A rectangular copper plate with an area of 76mm x 139.7 mm was brazed to a 6.4 mm O.D. tubing on the liquid side of the secondary evaporator to form this additional condenser. Cooling was achieved by bolting the two condenser plates together on a cold finger of a mechanical cryopump. The transport lines were gold plated. The pressure reduction reservoir was kept at room temperature during the testing, while the rest of the loop was enclosed in a nitrogen cooled shroud. The loop was instrumented with 18 Type T thermocouples. The Type T thermocouples were calibrated with readings from a high precision Lake Shore DT-670 silicon diode. The thermocouple locations are shown in Figure 8.

Several long duration tests were conducted. The main objectives of these tests were to demonstrate: 1) startup from a supercritical thermodynamic state; 2) operating in the temperature range of 20-30K; 3) a heat transport capability of 10W; 4) the ability of maintaining the loop operating temperature within 0.5K; and 5) a reliable operation. For testing, the shroud was cooled to 80 K, and then the cryocooler was turned on. Some test results are described below.

Start-up procedures for an initially supercritical loop were simple, straightforward, and reliable. Figure 10 shows the cool-down of the loop from the room temperature. Around 13:15, the cryocooler was turned on to cool the condensers. Temperatures of the cold finger and the condensers decreased steadily at the same rate. At 17:02, the cold finger temperature reached 30K, which was below the hydrogen critical temperature of 32K. The temperatures of the secondary pump dropped quickly but, at the same time, the secondary condenser temperature went up sharply. This indicated that as liquid was drawn into the secondary pump; superheated vapor from the hot reservoir was forced into the secondary condenser. At 17:08, the secondary condenser temperature started to decrease and eventually leveled off at 30K along with the secondary pump temperature at 17:20, suggesting that the secondary pump was filled with liquid or saturated fluid.

Over the next 4 hours, the primary pump and its CC, and the vapor line temperatures continued to drop very slowly. At 21:32, 2.5W was applied to the secondary pump to initiate a flow. Several events occurred subsequently: 1) The secondary evaporator temperature (TC13) rose and the liquid line temperature (TC9) dropped, indicating that a flow is initiated in the secondary loop; 2) The reservoir temperature (TC11) continued to drop because warm vapor was leaving toward the secondary condenser while cold fluid was drawn from the primary condenser; 3) The secondary condenser inlet temperature (TC15) initially increased because the warm fluid was drawn from the primary CC, then its temperature dropped along with the CC; 5) The primary evaporator temperature (TC2) dropped because the cold fluid from the primary condenser must flow through the evaporator core before it reached the CC and moved toward the secondary condenser. With the secondary loop running, the primary evaporator, CC, and the liquid line could be cooled very quickly.



Figure 9. Hydrogen CLHP in Thermal Vacuum Chamber

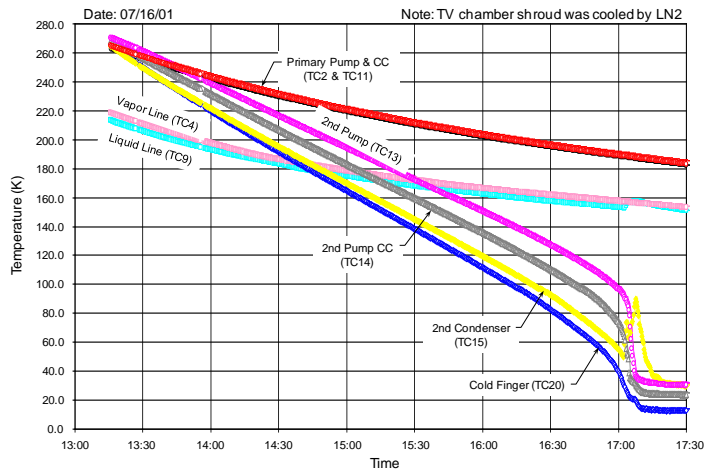


Figure 10. Initial Cooldown of Hydrogen CLHP

At 22:30, it was clear that a steady flow had been established in the secondary loop, and the primary loop was ready for startup. At 22:46, 2.5W was applied to the primary evaporator, and the primary loop started immediately as indicated by the drop of the vapor line temperature (TC4). The loop continued to operate steadily with 2.5W to the primary evaporator and 2.5W to the secondary evaporator as indicated in Figure 11.

Figure 12 shows another loop startup. After the secondary evaporator and the secondary condenser were cooled below the critical temperature, 2.5W was applied to the secondary evaporator to initiate a flow in the secondary loop. The subsequent events were similar to those shown in Figure 11. At 16:05, 5W was applied to the primary pump, and the primary loop started immediately.

In addition to facilitate the startup of the primary loop, the secondary loop can also compensate for the parasitic heat gain along the liquid return line. Figure 13 shows that the loop continued to operate steadily afterwards with 2.5W to the secondary evaporator and 5W to the primary evaporator after a successful startup. At 18:05, the heat load to the secondary evaporator was reduced to zero, and the primary loop operation degenerated to that of an ordinary LHP. The primary loop functioned well without the help from the secondary loop. This is because at a relatively high heat load (and mass flow rate) of 5W to the primary evaporator, the parasitic heat gain along the liquid line could be compensated for by the subcooled liquid returning to the CC. When the heat load to the primary evaporator was reduced to 1W at 19:20, however, the primary loop dried out due to insufficient subcooling to overcome the parasitic heat gain along the liquid line, i.e. the the reservoir temperature continued to rise above the critical temperature of hydrogen. An attempt was made to

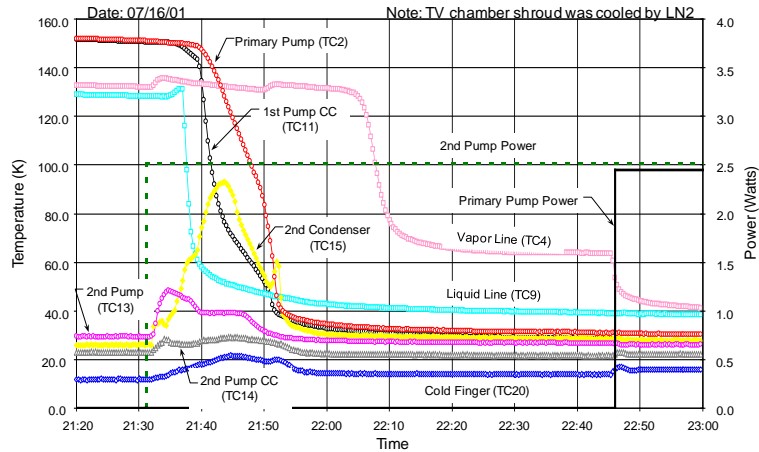


Figure 11. Startup of Hydrogen CLHP

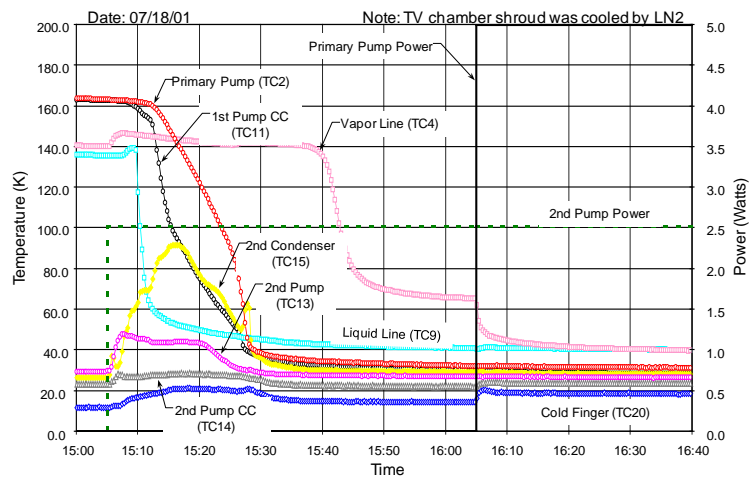


Figure 12. Startup of Hydrogen CLHP

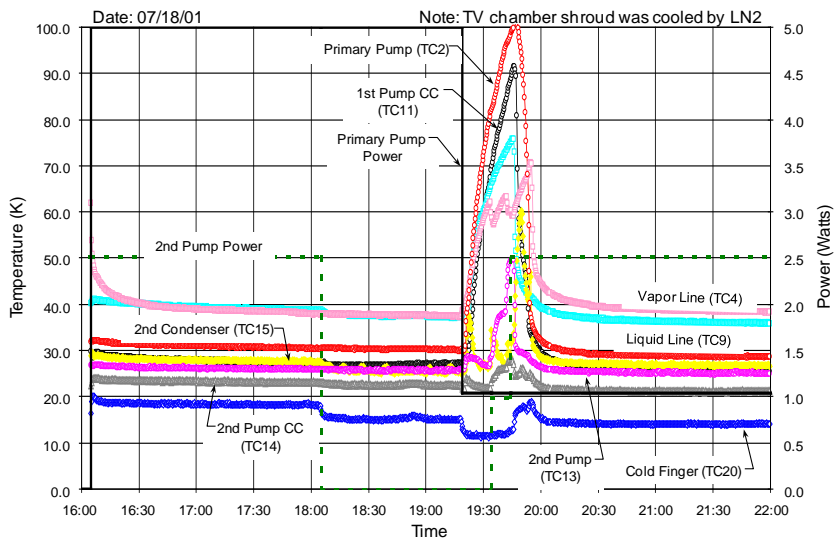


Figure 13. Dry-out and Recovery of Hydrogen CLHP

recover the loop by applying 1W to the secondary evaporator, which turned out to be insufficient to overcome the parasitic heat gain. By increasing the secondary evaporator power to 2.5W, the primary loop was completely recovered, and the loop operated steadily with 1W to the primary evaporator and 2.5W to the secondary evaporator.

Figure 11 and 12 show loop startup with 2.5W and 5W to the primary evaporator and secondary evaporator, respectively. In general, startup with low power is more difficult. A startup with 1W to the primary evaporator was tested and the loop temperature profiles are shown in Figure 14. Again, the events after 2.5W was applied to the secondary evaporator were similar to those shown in Figure 11. At 14:50, 1W was applied to the primary evaporator, and the primary loop was able to start without any difficulty.

Test was continued to study how low the heat load to the primary evaporator could be with 2.5W to the secondary evaporator, and how the loop would respond to a rapid change in the primary evaporator power. Figure 15 shows that the primary loop could operate with a heat load as low as 0.25W to the primary evaporator and 2.5W to the secondary evaporator. This illustrates the effectiveness of the secondary loop in compensating for the parasitic heat gain along the liquid line. Figure 15 also shows that the primary evaporator power could vary rapidly between 0.25W and 2.5W, achieving a turndown ratio of 10.

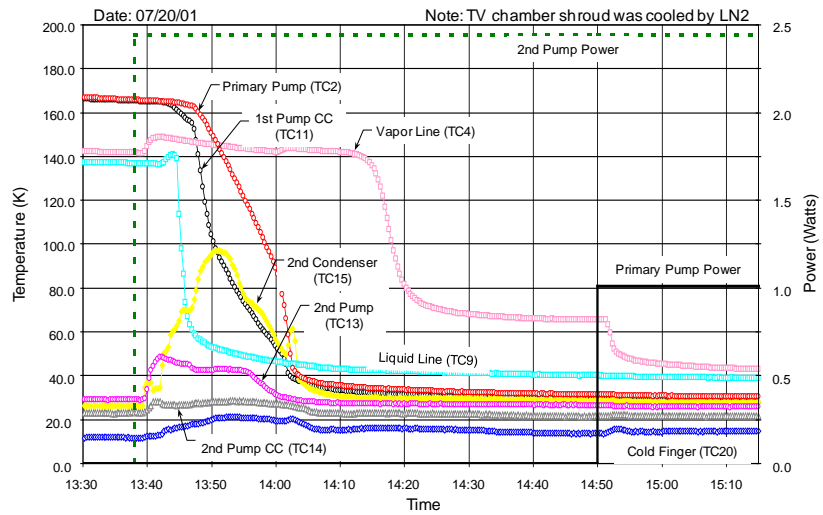


Figure 14. Low Power Startup of Hydrogen CLHP

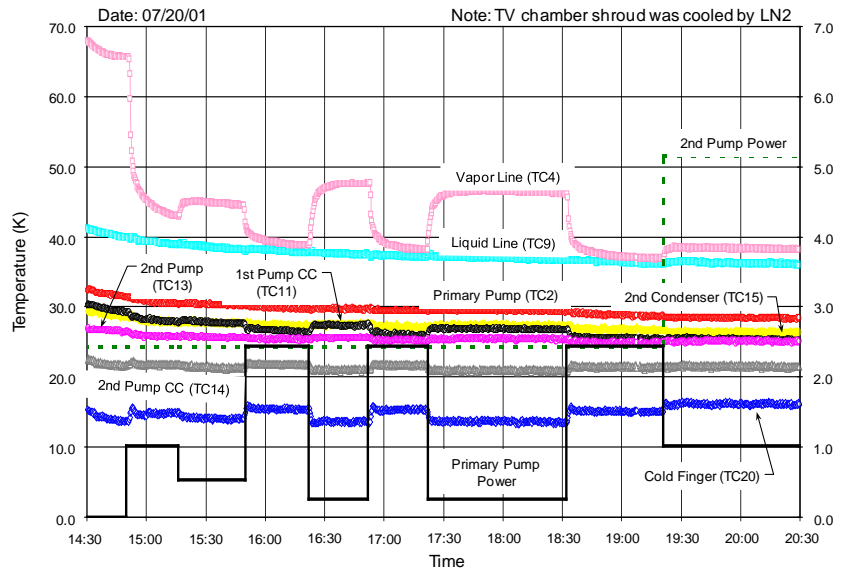


Figure 15. Power Cycle and Low Power Operation of Hydrogen CLHP

IV. Conclusions

Next generation space infrared sensing instruments and spacecraft will require drastic improvements in cryocooling technology in terms of performance and ease of integration. Projected requirements for cryogenic thermal control systems include high duty cycle heat loads, low parasitic heat penalty, long transport distances, highly flexible transport lines, and low cooling temperatures. All of these requirements can be satisfied by using a CLHP/cryocooler system. Adding a secondary evaporator to the traditional LHP solves the problems of parasitic heat gains and the difficulty of starting the loop from an initially supercritical state. The issue of a mismatch of coefficients between the evaporator shell and the primary wick can be resolved by using the same material. Adding a hot reservoir keeps the system pressure at a safe level at ambient temperature and at a subcritical level prior to the loop start-up.

Several CLHPs have been built and tested using nitrogen and hydrogen as working fluids, and these CLHPs demonstrated excellent performance in thermal vacuum tests. This paper described the performance of a hydrogen

CLHP in thermal vacuum testing. The loop demonstrated its reliable start-up, robust operation during transients of rapid power changes, low power operation and recovery from a dry-out condition.

References

1. Maidanik, Y., and Fershtater, Y., "Theoretical Basis and Classification of Loop Heat Pipes and Capillary Pumped Loops," *10th International Heat Pipe Conference*, Stuttgart, Germany, 1997.
2. Ku, J., "Operating Characteristics of Loop Heat Pipes," Paper No. 1999-01-2007, *29th International Conference on Environmental Systems*, Denver, Colorado, July 12-15, 1999.
3. Maidanik, Y., "Loop Heat Pipes – Theory, Experimental Developments and Application," *13th International Heat Pipe Conference*, Sydney, Australia, August 9-13, 2006.
4. Goncharov, K., Nikitkin, M., Fershtater, Y., and Maidanik, Y., "Loop Heat Pipes in Thermal Control System for OBZOR Spacecraft," *25th International Conference on Environmental Systems*, San Diego, California, July 10-13, 1995.
5. Grob, E., Baker, C., and McCarthy, T., "Geoscience Laser Altimeter System (GLAS) Loop Heat Pipe: An Eventful First Year On-Orbit", Paper No. 2004-01-2558, *34th International Conference on Environmental Systems*, Colorado Springs, Colorado, July 19-22, 2004.
6. Grob, E., "Performance of the GLAS Loop Heat Pipes – 7 Years in Orbit", Paper No. AIAA-2010-6029, *40th International Conference on Environmental Systems*, Barcelona, Spain, July 11-15, 2010.
7. Choi, M., "Thermal Assessment of Swift BAT Instrument Thermal Control System in Flight", Paper No. 2005-01-3037, *35th International Conference on Environmental Systems*, Rome, Italy, July 11-14, 2005.
8. Choi, M., "Thermal Assessment of Swift Instrument Module Thermal Control System during First 2.5 Years in Flight," Paper No. 2007-01-3083, *37th International Conference on Environmental Systems*, Chicago, Illinois, July 9-12, 2007.
9. Rodriguez, J. I., "Thermal Design of the Tropospheric Emission Spectrometer Instrument," Paper No. 2000-01-2274, *30th International Conference on Environmental Systems*, Toulouse, France, July 10-13, 2000.
10. Rodriguez, J. I., Na-Nakornpanom, A., Rivera, J., Mireles, V. and Tseng, H., "On-Orbit Thermal Performance of the TES Instrument – Three Years in Space," Paper No. 2008-01-2118, *38th International Conference on Environmental Systems*, San Francisco, California June 30 - July 2, 2008.
11. Nikitkin, M. and Wolf, D., "Development of LHP with Low Control Power," Paper No. 2007-01-3237, *37th International Conference on Environmental Systems*, Chicago, Illinois, July 9-12, 2007.
12. Ku, J., "Methods of Controlling the Loop Heat Pipe Operating Temperature," Paper No. 2008-01-1998, *38th International Conference on Environmental Systems*, San Francisco, California, June 30 - July 2, 2008.
13. Nikitkin, M. N., Kotlyarov, E. Y. and Serov, G. P., "Basics of Loop Heat Pipe Temperature Control", Paper No. 1999-01-2012, *29th International Conference on Environmental Systems*, Denver, Colorado, July 12-15, 1999.
14. Hoang, T., O'Connell, T., and Ku, J., "Advanced Loop Heat Pipes for Spacecraft Thermal Control," Paper No. AIAA-02-1266, *8th AIAA/ASME Joint Thermophysics and Heat Transfer Conference*, St. Louis, Missouri, June 24-27, 2002.
15. Hoang, T., T. O'Connell, and Ku, J., "Management of Parasitics in Cryogenic Advanced Loop Heat Pipes," Paper No. AIAA 2003-0346, *AIAA 41st Aerospace Sciences Meeting & Exhibit*, Reno, Nevada, January 6-9, 2003.
16. Hoang, T., O'Connell, T., Ku, J., Butler, B. and Swanson, T., "Miniature Loop Heat Pipes for Electronic Cooling," Paper No. 2003-35425, *International Electronic Packing Technical Conference and Exhibition*, Maui, Hawaii, July 6-11, 2003.
17. Ku, J., "Heat Load Sharing in a Loop Heat Pipe with Multiple Evaporators and Multiple Condensers," Paper No. AIAA-2006-3108, *9th AIAA/ASME Joint Thermophysics and Heat Transfer Conference*, San Francisco, CA, June 5-8, 2006.
18. Hoang, T., O'Connell, T.A., Khrustalev, D., and Ku, J., "Cryogenic Advanced Loop Heat Pipe in Temperature Range of 20-30 K," *12th International Heat Pipe Conference*, Moscow, Russia, May 19-24, 2002.